Vorticity Associated with a Jet in a Cross Flow

RICHARD FEARN* AND ROBERT P. WESTON†
University of Florida, Gainesville, Fla.

An extensive wind-tunnel test of a round turbulent jet directed normally through a flat plate into a subsonic cross flow has been conducted. The results of the velocity field measurements are presented in a concise and usable form through the use of simple models to relate the velocity field to empirical values for the strength and location of the pair of contrarotating vortices associated with the jet.

Nomenclature

a, b, c = curve-fitting parameters
D = diameter of jet orifice
$\hat{e}_{\theta_1}, \hat{e}_{\theta_2}, \hat{e}_{z_v}$ = unit vectors, see Fig. 2
h_o = half spacing of vortex centers for the diffuse vortex model
h = center of vorticity for the diffuse vortex model, or half spacing of vortices for the filament model
M_j = Mach number of jet fluid at orifice
M_∞ = Mach number of cross flow fluid
R = effective velocity ratio defined by Eq. (1)
r, r_1, r_2 = distances in vortex coordinate system, see Fig. 2
r_c = radius of vortex core defined by Eq. (6)
S_o = area of jet orifice
s = arc distance along vortex curve
U_j = speed of jet fluid at orifice
U_∞ = speed of cross flow fluid
U_c = speed of fluid at jet centerline
U_v, V_v, W_v = velocity components in the vortex coordinate system
X, Y, Z = wind-tunnel coordinate system (Cartesian), see Fig. 1
X_v, Y_v, Z_v = vortex coordinate system (Cartesian), see Fig. 1
β = diffusion constant, see Eq. (3)
Γ_o = integrated strength of each diffuse vortex defined by Eq. (5)
Γ = effective strength of each diffuse vortex, or strength of a vortex filament
γ_o, γ = dimensionless variables corresponding to Γ_o and Γ.
$\sum \gamma_i$ = flux of vorticity across each cross section, obtained by direct calculation from the measured velocity field
$\theta, \theta_1, \theta_2$ = angles in vortex coordinate system, see Fig. 2
ρ_j = mass density of jet fluid at orifice
ρ_∞ = mass density of cross flow fluid
ϕ_v = angle between Z and Z_v axes
ω_o = maximum vorticity of each diffuse vortex
ω = vorticity

Introduction

THE phenomenon of a turbulent jet of fluid directed normally or at a large angle into a cross flow occurs in numerous situations. Perhaps the most commonly observed example is that of smoke issuing from a chimney on a windy day. Recent investigations of a jet in a cross flow have been motivated by a variety of possible applications: the process of cooling combustion gases in gas turbine combustors[1]; the discharge of an effluent into a waterway[2]; and the aerodynamic problems encountered by VTOL aircraft in the transition between hover and wingborn flight.[3] It is the latter problem which motivated this study.

In an attempt to describe the essential features of the complicated flowfield encountered in the above problems, many investigators have concentrated their efforts on a standardized version of the problem; a round subsonic jet discharging through a large flat plate into a subsonic cross flow. Certain aspects of this problem, namely, the path of the jet and the pressure distribution on the flat plate, have been the subject of numerous investigations. By comparison, the pair of contrarotating vortices which constitutes the dominant feature of the velocity field has received much less attention until recently. An extensive bibliography for the jet in a cross flow with emphasis on applications to V/STOL aerodynamics is given by Margason[4] in a NASA special publication devoted entirely to this subject.

This paper reports on some of the results of an extensive experimental investigation of the velocity field associated with a jet in a cross flow. Two simple, two-dimensional models for the pair of contrarotating vortices associated with the jet are developed. The physical properties of the vortices are inferred from selected velocity measurements taken in cross sections perpendicular to the trajectory of the vortex pair. The physical properties of the vortices are presented for a range of jet to cross flow velocity ratios. This represents the first quantitative description of the pair of contrarotating vortices associated with a jet in a cross flow which includes their location, strength, and diffuseness.

Discussion of the Problem

The properties of a jet in a cross flow depend primarily on the ratio of the momentum flux across the jet orifice to the momentum flux of the cross-flow over an equal area. It is conventional to define an effective velocity ratio as the square root of this ratio of momentum fluxes

$$R = [\int_{S_o} \rho_j U_j^2 \, d\sigma / (\rho_\infty U_\infty^2 S_o)]^{1/2} \quad (1)$$

If the jet and cross flow fluids are the same and obey the ideal gas equation of state, and if the speed U_j is constant across the jet orifice and the pressure there is equal to the free stream pressure, then Eq. 1 simplifies to a ratio of jet to cross flow Mach numbers, $R = M_j/M_\infty$. If U_j is constant and $\rho_j = \rho_\infty$ as in the case of an unheated jet then Eq. (1) may be written simply as the ratio of the jet to cross flow velocities, $R = U_j/U_\infty$.

The path of the jet may be determined by flow visualization techniques, such as injection of smoke or water vapor into the jet, or by velocity measurements. In the latter case, the path of the jet is usually described by the jet centerline which is defined as the locus of points of maximum velocity in the symmetry plane.[1] The jet centerline may be detected to about 15 jet diam downstream of the jet orifice. Farther downstream there is not a measurable difference between the jet centerline speed and the cross flow speed. The pair of contrarotating vortices, however, are detectable much farther downstream. In this experiment, they were easily detected 45 jet diam downstream of the jet orifice. Pratt and Baines[5] report that they could detect the vortices up to 1000 jet diam downstream of the jet orifice. It would be useful to have a description for the path of the jet in terms of the location of this vortex pair. The projection of the vortex trajectories onto the symmetry plane ($Y = 0$) is defined

Received January 18, 1974; revision received May 28, 1974. This work was supported by NASA through Grant NGL 10-005-127.

Index categories: Aircraft Aerodynamics (Including Component Aerodynamics); VTOL Aircraft Design; Jets, Wakes, and Viscid-Inviscid Flow Interactions.

* Assistant Professor, Department of Engineering Sciences. Member AIAA.

† NSF Fellow, Department of Engineering Sciences. Student Member AIAA.

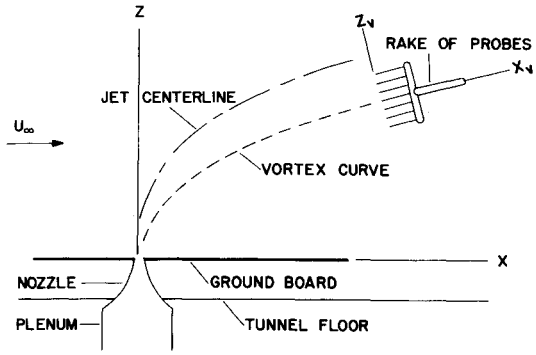

Fig. 1 Sketch of test apparatus and coordinate systems.

as the vortex curve and is shown in Fig. 1. The vortex coordinate system (X_v, Y_v, Z_v) is defined in terms of this curve which lies slightly below the jet centerline. In fact, the determination of a jet path by flow visualization probably coincides more closely with the vortex curve than with the jet centerline.

Recently, there have been two experimental investigations of the velocity field for a jet in a cross flow which complement the experiment described herein and provide comparisons for the results. In experiments by Kamotani and Greber[1] and by Thompson[3] the velocity measurements were taken in planes perpendicular to the jet centerline and vortex curve, respectively. Kamotani and Greber[1] present the measured velocity distribution in jet centerline cross sections as contours of constant velocity and as projections of the velocity vectors onto the plane of each cross section. This latter method clearly shows the presence of the vortices. Results of this nature are shown for two cross sections each for two effective velocity ratios. In addition to presenting the measured velocity field in the above manner for vortex curve cross sections, Thompson[3] attempts to infer the strength and the separation of the contrarotating vortices. He presents results for three different effective velocity ratios. The diameters of the jets used in the above experiments were $\frac{1}{4}$ in. and 1 in., respectively. These, together with the 4 in. diam jet used in this experiment, provide a Reynolds number range from 2.6×10^3 to 3.6×10^5 based on the freestream velocity and the jet diameter.

Experiment

The experimental investigation described herein was conducted in the V/STOL wind tunnel ($14\frac{1}{2}$ ft by 21 ft test section) at Langley Research Center, Hampton, Va., during three wind-tunnel tests between Dec. 1970 and Jan. 1973. Test section air speeds ranged from 100–175 fps. The jet of air was formed by using a plenum chamber and a 20:1 converging nozzle designed to provide a flat velocity profile at the 4 in. diam nozzle exit. Jet properties at the nozzle exit plane were calculated assuming isentropic flow from the plenum where total pressure and temperature were measured. Supply air for the jet was heated so that the temperature at the jet orifice would be the same as that of the cross flow. The jet discharged perpendicularly through a flat 4 ft by 9 ft ground board which was mounted 1 ft above the tunnel floor to avoid the tunnel boundary layer (see Fig. 1). The center of the jet was located 3 ft downstream of the rounded leading edge of the ground board.

Velocity determinations were made with a rake of seven yaw-pitch probes mounted on an airfoil with a 3 in. chord (see Fig. 1). The $\frac{1}{4}$ in. diam probes are 8 in. long, with a 2 in. spacing between probes. Each of the probes has a hemispherical tip with a total pressure port and a ring of 6 interconnected static ports 2 in. from the tip. To measure the angles of yaw and pitch, there are 4 pressure ports placed at approximately 45° to the total pressure port in the directions of yaw and pitch.

Because of the large flow angularity encountered in this experiment, the probes were calibrated experimentally through angles of 60°. Special calibration and data reduction schemes based on potential flow over a sphere were developed by Trovillion[6] to calculate the velocity at each probe tip from the six measured pressures. Based on the calibration data, which were taken in the wind tunnel before the jet and ground board were installed, the uncertainty in measuring flow direction ranged from less than $\frac{1}{2}$° for flow angularity of 10° or less to a maximum uncertainty of about 2° for larger flow angles. Similarly, the range of uncertainty in measuring the airspeed was from 1% to 5%. Errors due to turbulence were estimated from hot wire measurements at selected points in the jet. These errors and those due to velocity and pressure gradients in the flowfield were estimated to be within the range of the probe calibration errors and no attempt was made to correct for them.

The rake of yaw-pitch probes was used to measure velocities in planes approximately perpendicular to the vortex curve. A range of effective velocity ratios from 3–10 was studied from 2–45 jet diam downstream of the jet orifice. Velocity data for the simpler of the two vortex models consisted of a single placement of the rake of probes along the anticipated Z_v axis as shown in Fig. 1. The other vortex model required more detailed velocity data; velocities were measured at numerous points (35 to over 300) in a rectangular array for each of 20 cross sections. Although most of the velocity measurements were taken in the half plane $Y \geqq 0$, sufficient data were taken for $Y < 0$ to verify the assumption that the X-Z plane is a plane of symmetry for the velocity field. Additional velocity measurements were taken to verify the location of the jet centerline.

Vortex Models

A thorough experimental investigation of the velocity field would, of course, lead to a description of the vector vorticity field associated with the jet. The number of individual velocity measurements required for such a description, however, would be prohibitive. For example, over 300 velocity measurements were taken in the most extensively studied cross section, where it is estimated that 98% of the vorticity component perpendicular to the cross section is accounted for. To attempt this detail for numerous cross sections and for a range of effective velocity ratios would be a formidable task.

In this paper, two models are presented to describe quantitatively the contrarotating vortices associated with the jet. In each model, measured velocities in a vortex cross section are used to infer the component of vorticity perpendicular to that cross section. In the simpler model, the strength and the location of two infinite straight vortex filaments are determined by the measured upwash velocities along the Z_v axis. This two-dimensional vortex filament model is assumed to indicate the properties of the actual vortices at the location of the cross section. Although this model provides no description of the distribution of vorticity in the cross section, it has the distinct advantage of requiring relatively few velocity measurements. In the other model, the restriction that the vorticity be concentrated

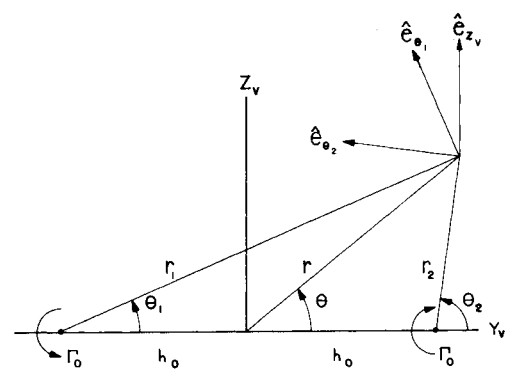

Fig. 2 Geometry for vortex models.

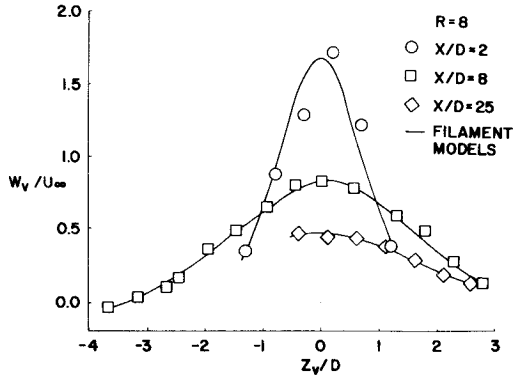

Fig. 3 Upwash velocities along the Z_v axis.

in a filament is relaxed and it is assumed that each vortex is composed of a Gaussian distribution of vorticity.[7] For this model, the strength, location and diffuseness of the vortex pair is determined by all of the measured upwash velocities in that cross section. A sketch of the geometry for the diffuse vortex model is shown in Fig. 2. It is assumed that the component of the freestream velocity in the plane of the cross section must be superimposed with that induced by the vortices to give the measured velocity.

In the vortex filament model, the upwash velocity along the Z_v axis may be written

$$W_v = \Gamma h/[\pi(h^2+Z_v^2)] - U_\infty \sin\phi_v \qquad (2)$$

where ϕ_v is the angle between the Z and Z_v axes; Γ and $2h$ are the strength and the separation between the two vortex filaments, respectively. The origin of the Z_v axis is located by the intersection of this axis with the line joining the two vortex filaments. It is at this point that the maximum upwash velocity occurs, and the locus of these points for all cross sections at a given effective velocity ratio defines the vortex curve. The circulation Γ, the half spacing h, and the origin of the Z_v axis are varied to obtain a least squares best fit[8] of Eq. (2) to the measured upwash velocities.

Figure 3 shows typical upwash velocity data along the Z_v axis on which the filament model is based. A single position of the rake provides sufficient data to infer the strength and the spacing of the vortex pair at a given cross section. It is noted that for large distances downstream of the jet the upwash velocity curve broadens and the span of seven probes eventually becomes inadequate to describe the curve. This is aggravated by the fact that the initial estimate of the vortex curve location was not very close in this region. The upwash, however, was detectable at cross sections 45 jet diam downstream of the orifice which was as far as measurements were taken. Also shown in Fig. 3 is the upwash velocity along the Z_v axis for a cross section where multiple rake positions provide more extensive data. It is seen that the filament model is able to describe the upwash velocities over a rather large range of Z_v. Data over such an extended range can be used to verify that the smaller sample of 7 velocity measurements spanning 3 jet diam is sufficient to determine the properties of the vortex filament pair.

In the diffuse vortex model, the approach is the same as for the filament model, but the distribution of vorticity within each of the contrarotating vortices is assumed to be Gaussian.[7]

$$\omega_{(r_1)} = \omega_o e^{-\beta^2 r_1^2} \quad \text{and} \quad \omega_{(r_2)} = -\omega_o e^{-\beta^2 r_2^2} \qquad (3)$$

The velocity at a point in the cross section is assumed to be induced by the superposition of these two diffuse vortices and the component of the freestream velocity in the plane of the cross section.

$$\mathbf{V} = \frac{\Gamma_o}{2\pi}\left[\left(\frac{1-e^{-\beta^2 r_1^2}}{r_1}\right)\hat{e}_{\theta_1} - \left(\frac{1-e^{-\beta^2 r_2^2}}{r_2}\right)\hat{e}_{\theta_2}\right] - U_\infty \sin\phi_v \hat{e}_{Z_v} \qquad (4)$$

where Γ_o is the integrated strength of each vortex distribution

$$\Gamma_o = \int_o^{2\pi}\int_o^\infty \omega_o e^{-\beta^2 r^2} r\, dr\, d\theta = \pi\omega_o/\beta^2 \qquad (5)$$

Any algebraic equation contained in the vector Eq. (4) could be used to determine the parameters of the model. For example, one could use the equation for the magnitude of the velocity or for one of the components of the velocity. After studying several possibilities, the equation for the Z_v component of the velocity has been chosen as the most suitable equation. The parameters Γ_o, h_o, and β can be determined at each cross section by fitting the velocity data with the equation for W_v using the method of least squares.[8] The effective strength of each vortex is taken to be the net flux of vorticity across the half plane $Y_v \leqq 0$ of the cross section

$$\Gamma = \int_{-\pi/2}^{\pi/2}\int_o^\infty \omega_{(r,\theta)} r\, dr\, d\theta$$

where

$$\omega_{(r,\theta)} = \omega_o(e^{-\beta^2 r_1^2} - e^{-\beta^2 r_2^2})$$

Because of the diffusion of vorticity across the symmetry plane, Γ may be less than Γ_o. The center of vorticity in ϕ and each half plane is defined by

$$h = \frac{1}{\Gamma}\int_{-\pi/2}^{\pi/2}\int_o^\infty Y_v \omega_{(r,\theta)} r\, dr\, d\theta$$

Evaluation of these integrals relates the effective strength and spacing of the vortices to the parameters of the model. The resulting expressions are: $\Gamma = \Gamma_o \operatorname{erf}(\beta h_o)$ and $h = h_o/[\operatorname{erf}(\beta h_o)]$, where

$$\operatorname{erf}(\beta h_o) = \frac{2}{(\pi)^{1/2}}\int_o^{\beta h_o} e^{-t^2} dt$$

is the error function. The effective strength and spacing (Γ and $2h$) of the vortices determined from the diffuse vortex model are assumed to be equivalent to the strength and spacing of the vortices determined from the filament model.

The diffusion constant β can be written in terms of a radius of the vortex core r_c defined as the distance from the center of a single Gaussian distribution of vorticity to the radius at which the maximum tangential speed occurs. The relation between the two parameters is

$$r_c/D = 1.121/\beta D \qquad (6)$$

Application of the vortex models required an iterative technique to achieve self-consistent results. From preliminary experi-

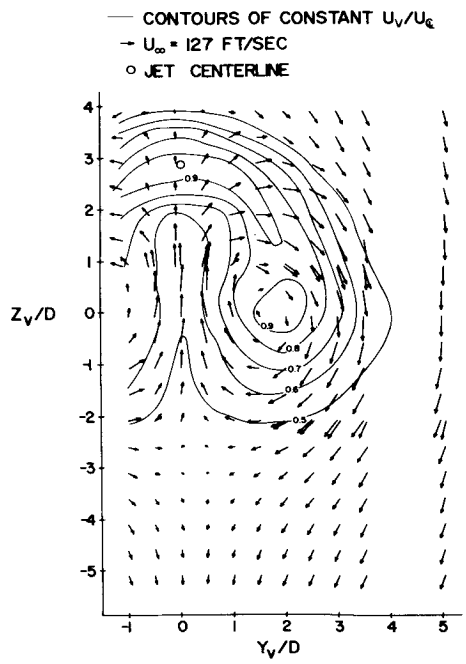

Fig. 4 Measured velocity field for cross section at $X/D = 5.2$ and $R = 8$.

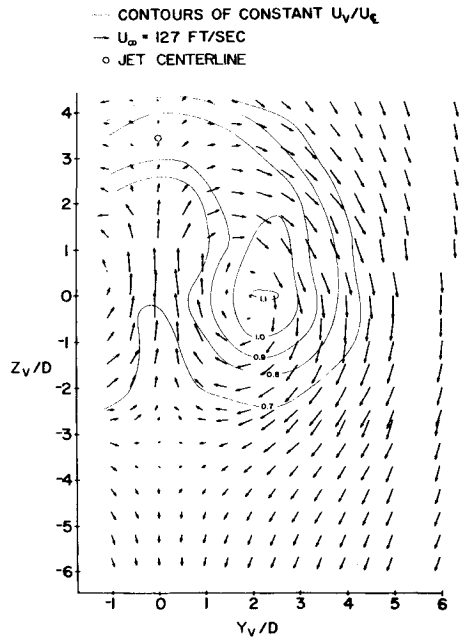

Fig. 5 Measured velocity field for cross section at $X/D = 8.3$ and $R = 8$.

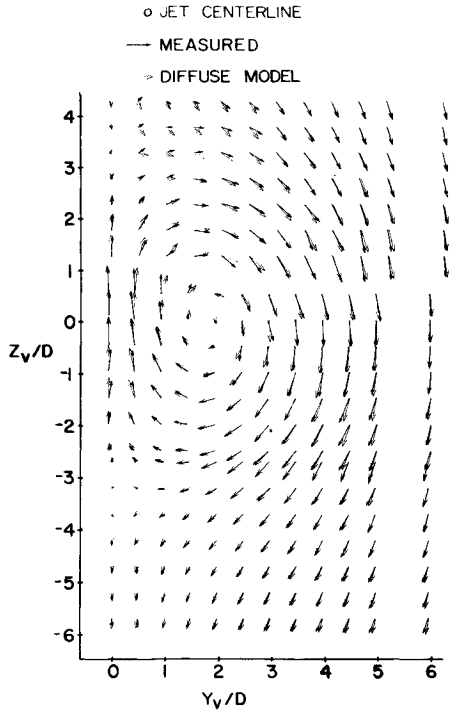

Fig. 6 Comparison of measured and calculated velocity fields for cross section at $X/D = 8.3$ and $R = 8$.

ments and from the results of Thompson,[3] a tentative description of the vortex curve as a function of effective velocity ratio was available. To obtain measured velocities for the filament model, the rake of probes was centered on the tentative vortex curve with the longitudinal axes of the probes parallel to the curve at that point. The measured velocities were resolved into components in a probe-fixed coordinate system and the upwash velocities were fit by Eq. (2) to determine the first approximation to the vortex parameters. The locus of these points for all maximum upwash velocities determined by the model for a given effective velocity ratio defined a new vortex curve. The measured velocites were next projected into a coordinate system defined by the revised vortex curve and this process was continued until there was a negligible change in the location of the vortex curve. The validity of this scheme depends on two things: A reasonably close initial description of the vortex curve and sufficiently weak axial (X_v) gradients of the velocity. In this experiment, the final vortex cross section was usually within a few degrees of the cross section in which the data were taken. It is also found that the properties of the vortex pair as determined by the vortex models are relatively insensitive to small angle rotations of the cross section onto which the measured velocities are projected. For example, a rotation of the most extensively studied cross section through an angle of $\pm 5°$ changes the value of Γ only about 3%.

Results

The measured velocity fields at two cross sections for an effective velocity ratio of 8 are presented in Figs. 4 and 5. An attempt to display the three-dimensional velocity for each cross section is made by superimposing contours of constant U_v (velocity component perpendicular to the cross section) on a vector plot of the projection of the velocity onto the cross section. In Fig. 4, the jet centerline speed is $U_C = 1.89\ U_\infty$ and the component of the cross flow velocity perpendicular to the cross section is $(U_\infty/U_C)\cos\phi_v = 0.444$. For Fig. 5, $U_\zeta = 1.46\ U_\infty$ and $(U_\infty/U_\zeta)\cos\phi_v = 0.616$. From these numbers, one can see the extent of the jet as evidenced by the contours of constant U_v/U_ζ. Also note that the X_v component of the velocity decays more slowly in the vortex core than at the jet centerline location.

The degree to which the diffuse model describes the measured velocity field in the most extensively studied cross section (Fig. 5) is illustrated in Fig. 6. The lightweight arrows are the velocities calculated from the diffuse vortex model so that when only a heavy arrow shows, the velocity calculated by the model coincides with measured velocity. The top three rows of velocities are in the neighborhood of the jet centerline and are not

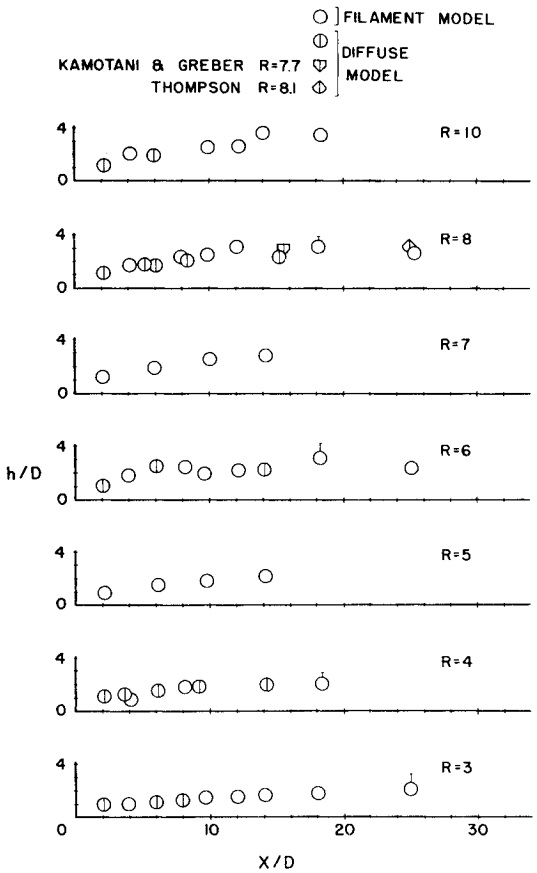

Fig. 7 Vortex spacing.

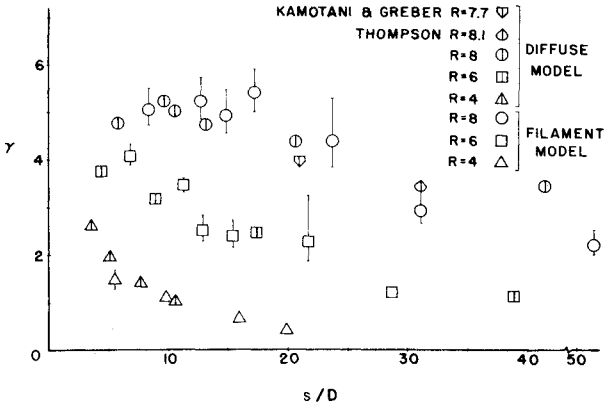

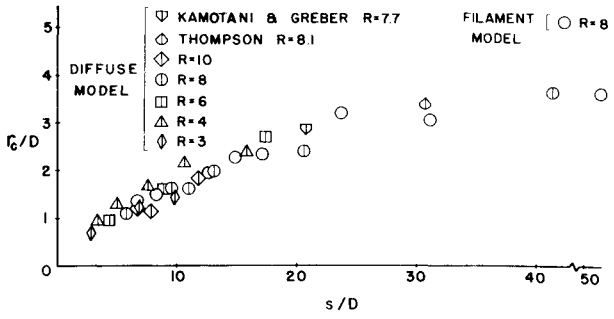

Fig. 9 Vortex core size.

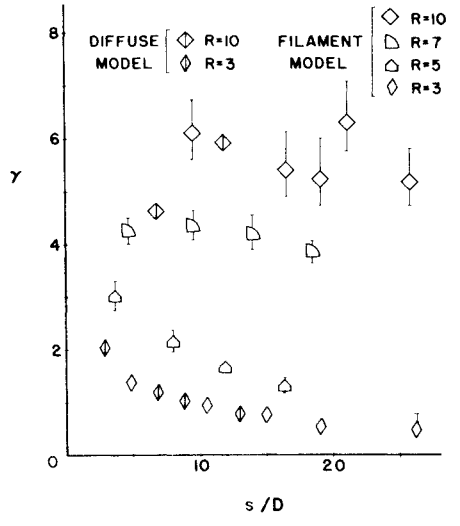

Fig. 8 Vortex strength. a) $R = 4$, 6, and 8. b) $R = 3$, 5, 7 and 10.

used in determining the model parameters. For the rest of the cross section, the diffuse vortex model describes the projection of the velocity field onto the cross section remarkably well.

The results of applying the two vortex models to the measured velocity field are shown in Figs. 7–10. Comparison with the results in Kamotani and Greber[1] and with Thompson[3] is made by using velocity data from these two experiments in the diffuse vortex model. Figure 7 shows the vortex spacing and Fig. 8 shows the variation of the vortex strength with arc distance along the vortex curve for a range of effective velocity ratios. The vortex strength obtained from Thompson's data is within 5% of the value that he estimated for this location. The vortex strength is nondimensionalized by the value one would obtain for a roll up of the vorticity associated with two-dimensional potential flow around a circular cylinder, into a pair of contrarotating vortices as described by Chang-Lu[9]; $\gamma = \Gamma/2DU_\infty$. The uncertainties of the vortex separation and strength in the filament models (Figs. 7 and 8) are obtained by assuming that the velocity data are scattered randomly about the upwash velocity curve, Eq. (2). The curve is deformed in such a manner as to cause maximum changes in the vortex separation and strength; the deformation of the curve at any point being limited to the probable error of the data.

Table 1 presents the results of the diffuse vortex model at six cross sections for an effective velocity ratio of 8. Each cross section is located by its intersection with the vortex curve (X/D, Z/D). The extent of each cross section is indicated by the ratio of the vortex strength obtained by direct summation of the vorticity ($\sum\gamma_i$) calculated from the measured velocity field to the effective vortex strength determined from the model. Also, the number of measured velocities (No. pts.) used to determine the model parameters is given for each cross section. The degree to which the diffuse model is able to fit the velocity data in each cross section is indicated by the rms fit to both the Z_v and Y_v velocity components. Figure 6 provides a visual reference for the significance of these numbers. Also presented in Table 1 are the results of the diffuse vortex model with the constraint that γ_o is constant at the value determined by the largest cross section. Note that the degree to which the model fits the data for these two approaches is about the same. Even when measurements were taken over an area too small to determine the diffuse model parameters adequately, it appears that reasonable values are obtained for the effective vortex strength and spacing.

The results of this experiment suggest a modification of the qualitative description of the jet in a crossflow given by Pratte and Baines.[5] In a region very near the jet orifice, the vortex pair is formed, that is, values for γ_o, h_o, and β are established. Thereafter, it is consistent with the data from this experiment to assume that γ_o is constant and that the pair of contrarotating vortices spread (increase in h_o) and diffuse (decrease in β) in such

Table 1 Diffuse vortex model parameters, $R = 8$

						Fit to γ_o, h_o, and β					$\gamma_o = 5.63$ Fit to h_o and β					
X/D	Z/D	$\frac{\sum\gamma_i}{\gamma}$	No. pts	rms[b] fit to W_v	rms[b] fit to V_v	γ_o	γ	h_o/D	h/D	r_c/D	rms fit to W_v	γ	h_o/D	h/D	r_c/D	ϕ
2.13	4.87	0.61	49	5.6%	5.5%	5.95	4.77	0.92	1.15	1.13	5.6%	4.71	0.96	1.15	1.09	
5.21	7.58	0.94	135	3.8%	4.2%	7.10	5.23	1.34	1.81	1.90	4.2%	4.96	1.62	1.84	1.64	
5.99	8.03	0.56	36	5.0%	6.9%	12.11	5.01	0.69	1.66	2.00	5.5%	4.63	1.38	1.68	1.62	
8.34[a]	9.12	0.98	216	3.0%	3.6%	5.63	4.72	1.75	2.09	1.98	3.0%	4.72	1.75	2.09	1.98	
15.21	11.88	0.69	140	4.1%	7.2%	5.19	4.36	2.04	2.42	2.29	4.1%	4.45	1.91	2.41	2.41	
35.5	16.2	0.16	49	5.8%	4.6%	4.27	3.44	2.70	3.36	3.30	5.8%	3.70	2.22	3.38	3.71	

[a] Reference cross section.
[b] Expressed as a percentage of the maximum upwash velocity induced by the vortex system.

Table 2 Diffuse vortex strengths

R	No. cross sections	Total no. pts.	γ_o
3	3	112	2.2
4	5	244	2.8
6	3	119	4.5
8	6	625	5.6
10	2	96	7.0

a manner that they gradually weaken each other (decrease in γ). If this description is valid, one could use the diffuse model at a particular cross section to determine the value of the parameter γ_o. The vortex filament model which determines γ and h, and requires much less experimental input, could then be used to infer h_o and β for other cross sections in the following manner: calculate βh_o from $\text{erf}(\beta h_o) = \gamma/\gamma_o$; then $h_o = \gamma h/\gamma_o$ and $\beta = (\beta h_o)/h_o$. The core size is given in terms of β by Eq. (6).

The cross section at $X/D = 8.3$ with $R = 8$ is the only one in this experiment which contains enough information to determine γ_o adequately. For the other velocity ratios, however, γ_o can be estimated by utilizing the data from all cross sections at which data were taken for the diffuse model for that velocity ratio. A least squares fit to these data provides a single value of γ_o and values of β and h_o for each cross section. The results of these calculations are shown in Table 2; they indicate the linear relation $\gamma_o = 0.7\ R$. This unexpected result has an interesting implication. For this experiment, the initial strength of each vortex can be written $\Gamma_o = 1.4\ DU_j$, i.e., the initial strength of each vortex appears to be directly proportional to the speed of the jet at the orifice and to the diameter of the jet.

Figure 9 shows the values for the core size of the vortices as a function of arc length along the vortex curve. In addition to the filament model and the diffuse model results for an effective velocity ratio of 8, some results are shown for other velocity ratios. These data demonstrate that the vortices diffuse at a rate which is a function of arc length along the vortex curve, but only a weak function of R.

Since the customary method of describing the path of the jet has been in terms of the jet centerline, it may be useful to provide a description of both the jet centerline and the vortex curve. Although a more complex equation for the vortex is used in the vortex models, both the jet centerline and the vortex curve may be described adequately by an equation of the form $Z/D = aR^b(X/D)^c$. A least squares fit of the centerline and vortex curve locations for all effective velocity ratios studied provides the following values for the parameters: vortex curve, $a_v = 0.3473$, $b_v = 1.127$, $c_v = 0.4291$; jet centerline, $a_c = 0.9772$, $b_c = 0.9113$, $c_c = 0.3346$. The vortex curve is shown in Fig. 10 and the jet centerline is shown in Fig. 11. In both figures, numerous data points are not shown because they coincide with those plotted.

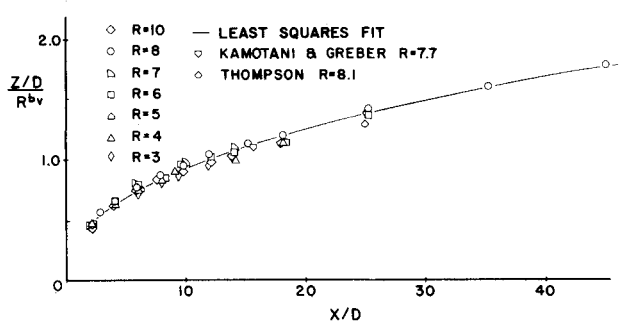

Fig. 10 Vortex curve.

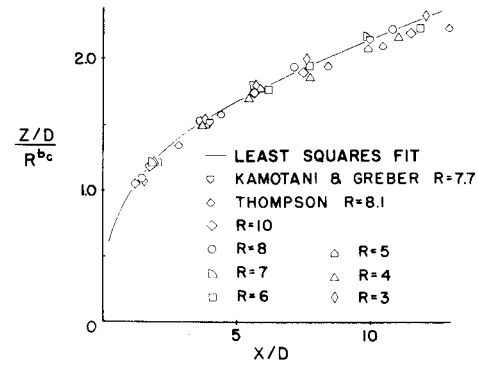

Fig. 11 Jet centerline.

Conclusion

The results of this experiment indicate that the dominant feature of the velocity field for a jet in a cross flow is a pair of contrarotating vortices. Once this is realized, it is evident that certain physical parameters are required for their description: the strength, the location, and a measure of the diffuseness. From this point, the development of the two vortex models is straightforward and the parameters describing the vortices are determined by the measured velocity field. These models provide the following description of the vortices: The vortex pair is formed very close to the jet orifice as relatively concentrated vortices with an initial strength that is directly proportional to the speed of the jet at the orifice and to the diameter of the jet. The vortices are deflected by the cross flow and they diffuse at a rate which is a function of the arc length along the vortex curve, but which is a weak function of the effective velocity ratio. The vortices gradually weaken each other by the diffusion of vorticity across the symmetry plane.

Additionally, these vortex models provide a straightforward and reasonably simple method to reconstruct the velocity field induced by the pair of contrarotating vortices associated with a jet in a cross flow.

References

[1] Kamotani, Y. and Greber, I., "Experiments on a Turbulent Jet in a Cross Flow," *AIAA Journal*, Vol. 10, No. 11, Nov. 1972, pp. 1425–1429.

[2] Campbell, J. F. and Schetz, J. A., "Flow Properties of Submerged Heated Effluents in a Waterway," *AIAA Journal*, Vol. 11, No. 2, Feb. 1973, pp. 223–230.

[3] Thompson, A. M., "The Flow Induced by Jets Exhausting Normally from a Plane Wall into an Airstream," Ph.D. thesis, 1971, Univ. of London, London, England.

[4] Margason, R. J. and Fearn, R. L., "Jet-Wake Characteristics and Their Induced Aerodynamic Effects on V/STOL Aircraft in Transition Flight," SP-218, Sept. 1969, pp. 1–18, NASA.

[5] Pratte, B. D. and Baines, W. D., "Profiles of the Round Turbulent Jet in a Cross Flow," *Journal of the Hydraulics Division, Proceedings of the ASCE*, Vol. 92, No. HY6, Nov. 1967, pp. 53–64.

[6] Trovillion, T. A., "Experimental Investigation of the Velocity Field of a Jet in a Crossflow," M.S. thesis, 1972, University of Florida, Department of Engineering Sciences, Gainesville, Fla.

[7] Lamb, H., *Hydrodynamics*, 6th ed. Dover, New York, 1932, pp. 591–592.

[8] Nielsen, K. L., *Methods in Numerical Analysis*, 2nd ed. Macmillan, New York, 1964, pp. 308–311.

[9] Chang-Lu, H., "Aufrollung eines Zylindrischen Strahles durch Querwind," Ph.d. dissertation, Univ. of Göttingen, Göttingen, F.R., Germany, 1942.